International Journal of Heat and Mass Transfer 149 (2020) 119180

Contents lists available at ScienceDirect

International Journal of Heat and Mass Transfer

journal homepage: www.elsevier.com/locate/hmt

Fabrication and evaluation of a high-performance flexible pulsating heat pipe hermetically sealed with metal

Chuljae Jung, Jonghyun Lim, Sung Jin Kim*

Department of Mechanical Engineering, Korea Advanced Institute of Science and Technology, 291 Daehak-ro, Daejeon 305-701, Republic of Korea.

ARTICLE INFO

Article history:
Received 26 August 2019
Revised 22 November 2019
Accepted 6 December 2019
Available online 17 December 2019

Keywords:
Pulsating heat pipe
Flexible heat spreader
Thermal performance
Long-term reliability
Silane-mediated bonding method

ABSTRACT

A high-performance flexible pulsating heat pipe (FPHP) hermetically sealed with metal has been developed as a flexible heat spreader. For this, experimental works are conducted to evaluate the thermal performance and long-term reliability of the FPHP. The FPHP consisted of a polycarbonate sheet and flexible-copper-clad-laminates (FCCLs). Rectangular channels with dual hydraulic diameters of 0.75 mm and 0.5 mm were engraved on the polycarbonate sheet. The width, length, and thickness of the FPHP were 53.4 mm, 85.5 mm, and 0.64 mm, respectively. To prevent the permeation of non-condensable gases (NGCs) from the ambient, the upper and lower sides of the channel wall were encapsulated with the copper side of the FCCLs by a silane-mediated bonding method, and the flanges of the FPHP were sealed by soldering the two copper-foils. As the working fluid, HFE-7000 was charged into the FPHP. The FPHP has a maximum effective thermal conductivity of 1070 W/m·K, which is approximately 2.7 times higher than that of copper in the vertical orientation. The effective thermal conductivity of the FPHP decreases by 20.4% and 3.4% for the horizontal orientation and 45-degree bent condition, respectively. The long-term reliability of the FPHP was evaluated by measuring its gas permeability. The results show that the rate of the pressure increase inside the FPHP is approximately 0.54 Pa/day, indicating that the lifetime of the FPHP is at least 2000 days. The proposed method enables the fabrication of a thin and flexible pulsating heat pipe with high thermal performance and guaranteed long-term reliability.

1. Introduction

As the performance of electronic devices has improved, the heat generated by electronic devices has increased as well. Therefore, to assure their performance and long-term reliability, thermal management of electronic devices has become an integral part of their development. Moreover, with the trend toward flexible electronic devices, such as wearable devices and bendable phones, there is an increasing need for a flexible heat spreader for effective cooling of flexible devices. As a candidate for a flexible heat spreader, a pulsating heat pipe (PHP), which was proposed by Akachi et al. [1], has been attracting attention due to its simple structure and high performance. PHPs consist of meandering channels without any wick structure required of conventional heat pipes.

During the last two decades, polymers, due to their low Young's modulus, have been used as base materials of flexible PHPs (FPHPs) [2,3]. However, there exist two inherent problems associated with these FPHPs. First, their thermal performance deteriorates in less than a day due to the high gas permeability of polymers. This is because non-condensable gases (NCGs) disturb the condensation phenomena, decreasing the driving force of PHPs [4–6]. To prevent the permeation of NCGs from the ambient, a new type of FPHP was suggested in which a polymer sheet engraved with micro-channels is packaged with two metallic films [7–9]. Lim and Kim [9] fabricated a FPHP in which multilayer laminated films were attached on the upper and lower sides of the channel wall and indium was coated on the flanges of the FPHP. With metallic packaging, the thermal performance of the FPHP is maintained for 306 days. However, this is still too short compared to the lifetime of electronic devices. The main reason for the insufficient lifetime of the FPHP is that polymer layers in the flanges are partially exposed to the ambient. Therefore, it is necessary to improve the long-term reliability of FPHPs by using a bonding method in which the flanges of FPHPs are hermetically sealed with metal.

Second, unlike PHPs made of metal or silicon [10–13], the thermal performance of FPHPs still remains at the level of copper. The low thermal performance of FPHPs can be attributed to the method of bonding the base material and envelope. Existing bonding methods for fabricating FPHPs, such as adhesive bonding [7,8] or thermal bonding [9], are not suitable for FPHPs with micro-channels, because the micro-channels can be easily clogged by the

* Corresponding author.
E-mail address: sungjinkim@kaist.ac.kr (S.J. Kim).

https://doi.org/10.1016/j.ijheatmasstransfer.2019.119180
0017-9310/

Nomenclature

A_c	cross-sectional area [m^2]
D_{crit}	critical diameter [m]
g	gravitational acceleration [m/s^2]
I	electric current [A]
k	thermal conductivity [W/m·K]
L	length [m]
P	pressure [Pa]
Q_{in}	input power [W]
t	time [s]
T	temperature [°C]
$\overline{T}$	time-averaged temperature [°C]
V	electric voltage [V] or volume [m^3]

Greek Symbols

ρ	density [kg/m^3]
σ	coefficient of surface tension [N/m]

Subscripts

a	adiabatic section
c	condenser section
e	evaporator section
eff	effective
f	liquid phase
FPHP	flexible pulsating heat pipe
g	vapor phase
system	system

adhesive or melted polymer [14,15]. A clogging problem can not only reduce the hydraulic diameter of the channel but also deform the cross-sectional shape of the channel from a square to a circle. Generally, it is known that such changes in the channel geometry deteriorate the thermal performance of PHPs [16–18]. Therefore, it is necessary to improve the thermal performance of FPHPs by using a bonding method that does not deform the channel geometry.

The purpose of the present study is to improve the long-term reliability and the thermal performance of FPHPs. To achieve this, a new fabrication process of FPHPs is proposed. The proposed fabrication process enables FPHPs to be hermetically sealed with metal and prevents the channel geometry from being deformed. To evaluate the thermal performance and long-term reliability of the FPHP, a series of experiments are conducted. The thermal performance of the FPHP is measured at various input powers in three conditions: vertical orientation, horizontal orientation, and 45-degree bent condition. In addition, the long-term reliability of the FPHP hermetically sealed with metal is evaluated by using the pressure rise method [19] to measure the gas permeability of the FPHP.

2. Experiments

2.1. Fabrication of FPHPs

To fabricate a FPHP, polycarbonate (PC), which is flexible, was used as a base material and wrapped in flexible-copper-clad-laminates (FCCLs), as presented in Fig. 1. Using a picosecond laser, a dual-diameter channel with 15 turns was formed in the PC sheet, as shown in Fig. 2(a). The widths of the channel were 0.5 mm and 1.5 mm, and the height of the channel was 0.5 mm, which are optimal values for maximizing the figure of merit suggested by Kwon and Kim [13]. The FCCL consists of two layers, as shown in Fig. 2(b). The outermost layer is a polyimide (PI) film with good mechanical and chemical stability that serves as a protective layer. The bottom layer is a copper-foil that acts as a gas-barrier layer which is essential for all two-phase heat transfer devices in that NCGs interfere with the condensation of the working fluid. To bond the PC sheet and the copper-foil of the FCCL, the silane-mediated bonding [20] was carried out with some modifications. Using silane coupling agents, the surface of the PC sheet was chemically modified and then bonded to the copper-foil of the FCCL at a room temperature [21].

The detailed bonding process is depicted in Fig. 3. The surface of the PC sheet, on which the channel was formed, was cleaned thoroughly with isopropyl alcohol (IPA, 99%) and dried under a stream of nitrogen. Then, it was treated with oxygen plasma (Asher

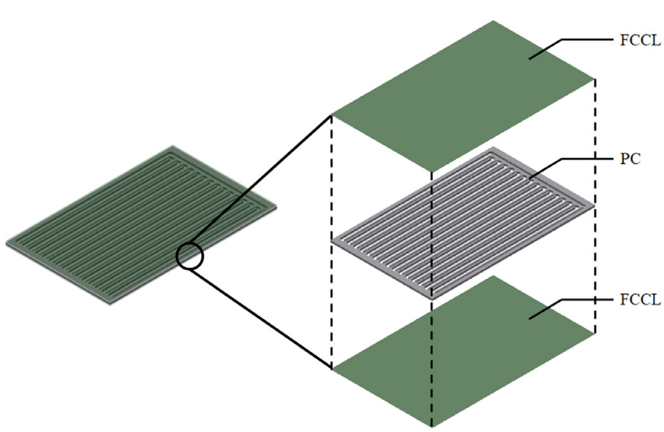

Fig. 1. Schematic of the FPHP.

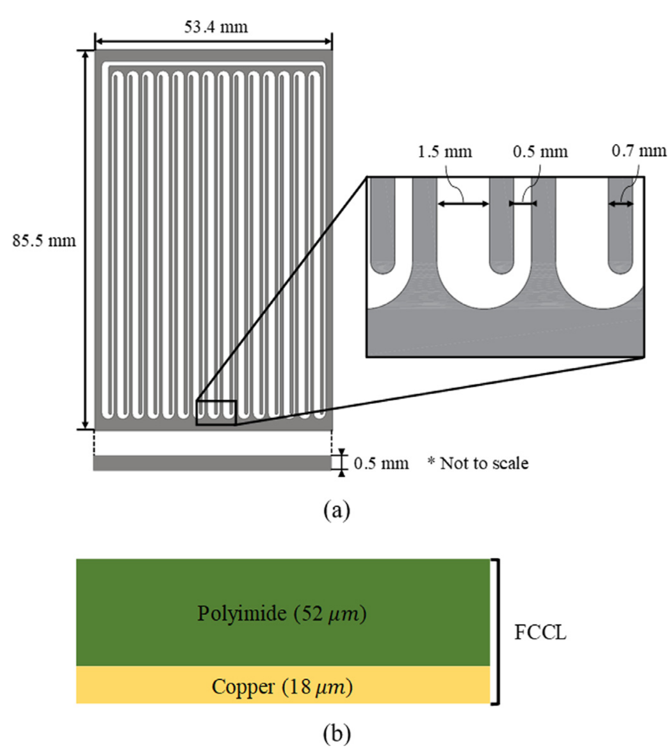

Fig. 2. Schematics of the (a) base and (b) envelope.

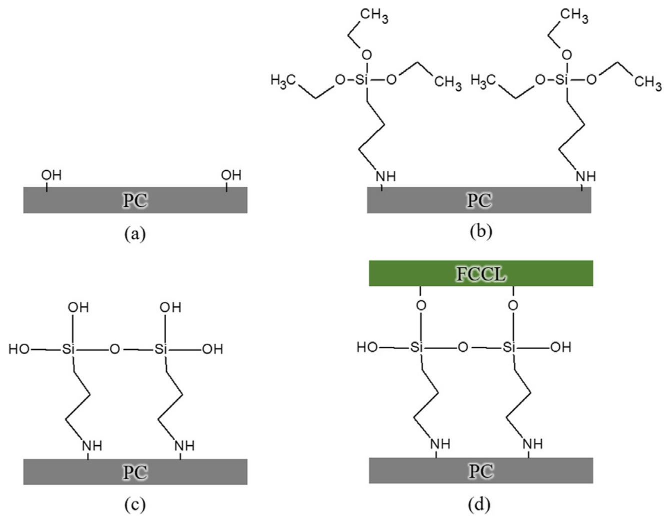

Fig. 3. Fabrication process for bonding PC to FCCL using silane coupling agent: **(a)** oxygen plasma treatment, **(b)** silane coating, **(c)** curing, and **(d)** silane-mediated bonding.

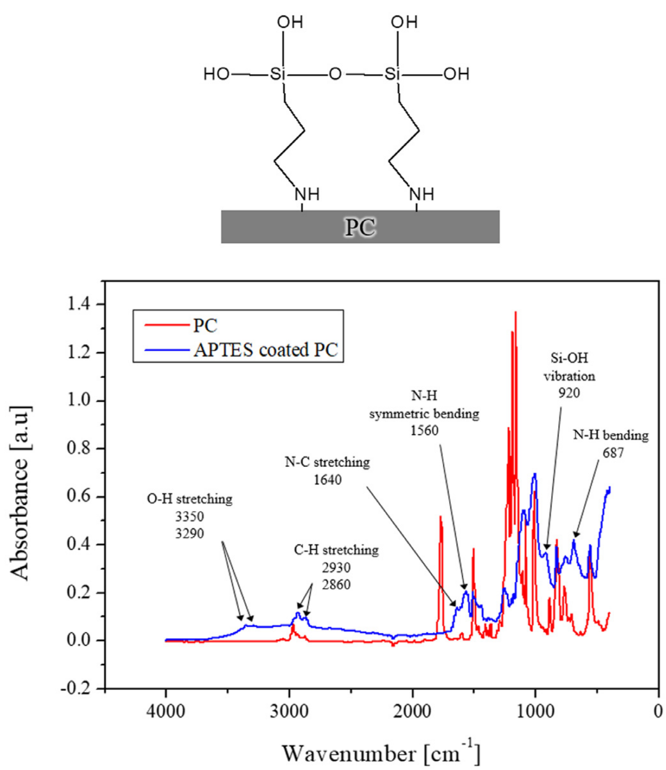

Fig. 4. FTIR transmission spectra of PC before and after treatment with APTES.

system; ULTEC, Inc.) (Fig. 3(a)). The plasma activated surface contained hydroxyl groups which were subsequently combined with molecules of the silane coupling agent. After that, the PC sheet was immediately immersed in a solution of 5 wt% silane in IPA. Amino-propyl-triethoxy-silane (APTES) was used as the silane coupling agent. After removing excess silane solution, the coated surface of the PC sheet was thoroughly dried under a stream of nitrogen (Fig. 3(b)). To cure the coating, the coated surface was placed in a convection oven at 70 °C for 30 min to 1 h At this point, APTES molecules, which are independent of each other, react with moisture and are cured (Fig. 3(c)). When surface modification of the PC sheet is ideally completed, rainbow bands can be seen on the surface. Fig. 4 shows the types of atomic bond on the surfaces of the APTES-coated PC and the pristine PC using the Fourier transform infrared (FTIR) spectroscopy. In this graph, the types of atomic bond on the surface were determined by the wave number when the peak value exists. It can be seen that several peaks were produced after the PC surface had been treated with the APTES. The peak at 1640 cm^{-1} was attributed to the N−C group [22], which means that APTES was well bonded to the surface. The peak at 920 cm^{-1} was attributed to the Si-OH group [23], which means the curing process was carried out very well. This is because the Si-OH group was created in response to water molecules. After coating, the coated surface of the PC sheet was treated with oxygen plasma. Also, the copper surface of the FCCL was treated with oxygen plasma. These two surfaces were attached to each other and cured at a room temperature for 24 h using a hot press (QMESYS, Inc.) (Fig. 3(d)). Using the same process, the other side of the PC sheet was bonded to the copper-foil of the FCCL.

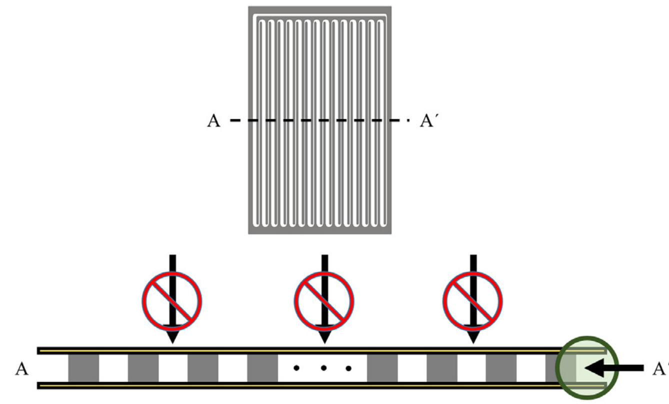

Fig. 5. Gas permeation from the ambient into the channel through the flanges of the FPHP.

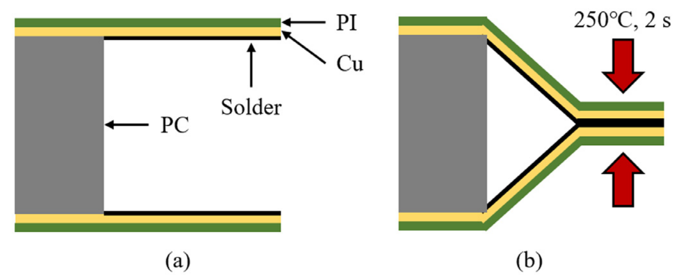

Fig. 6. Schematics of bonding process in the flanges of the FPHP: (a) tinning and (b) hot-pressing.

The FCCL enveloping the channel can effectively block gas permeation from the ambient to the upper and lower sides of the channel. However, as shown in Fig. 5, NCGs can still permeate into the channel through the flanges of the FPHP. Lim and Kim [9] showed that gas permeation through the flanges had a significant effect on the long-term reliability of the FPHP. It has been reported that the long-term reliability of the FPHP was improved 2.6 times by sealing the flanges of the FPHP with indium. In the present study, the flanges were hermetically sealed by soldering the two copper-foils. The bonding process is as follows (Fig. 6): first, the copper surfaces, which were the innermost layer, were rinsed thoroughly with ethanol, and then roughened using sandpaper. Then, solder was coated on the copper surfaces (Fig. 6(a)). Finally, the two parts were pressed at 250 °C for just 2 s (Fig. 6(b)). Fig. 7 provides SEM images of the cross-section of the joint. It can be seen that there is no void at the interface of the copper and the solder layers. Fig. 8 shows a FPHP fabricated using the above men-

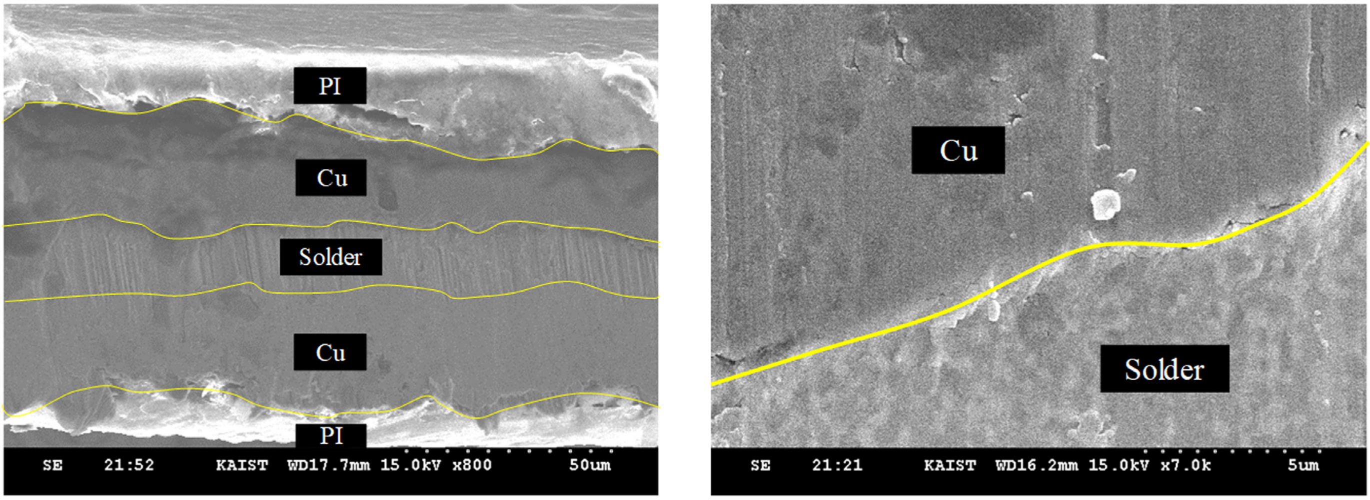

(a) (b)

Fig. 7. (a) 800 times and (b) 7000 times magnification SEM images of the cross-section of the flange joint.

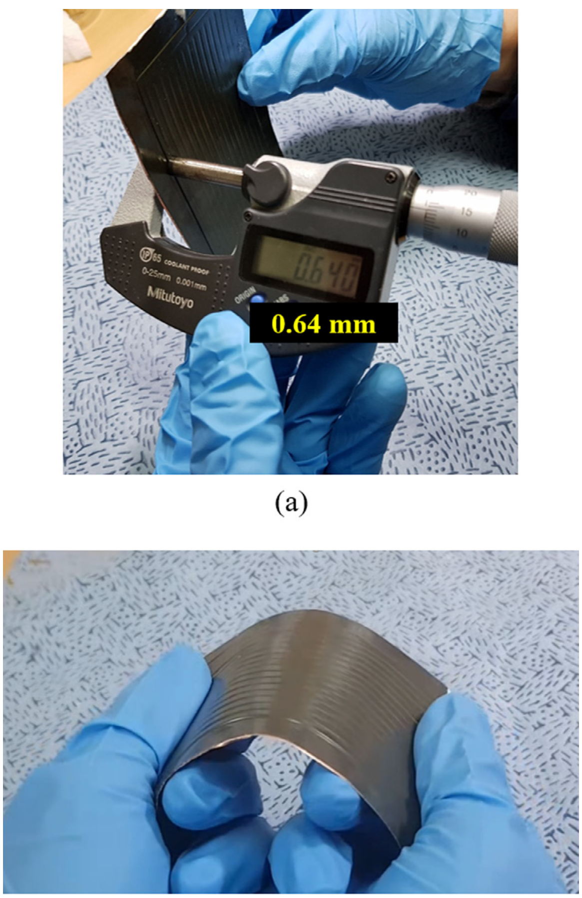

(a)

(b)

Fig. 8. Photographs of the FPHP: (a) thickness of the FPHP and (b) the FPHP under bent condition.

tioned process. The FPHP has a total thickness of 0.64 mm and is literally flexible.

After fabrication process was completed, a leak test was performed using a helium leak detector (VSMR152, Agilent Technologies, Inc.). No helium was detected, even at a rate of 10^{-10} atm·cc/s. Then, the interior of the FPHP was evacuated to less than 10^{-3} Torr and charged with the working fluid through a hole on the upper side. HFE-7000 was selected as the working fluid, and dissolved non-condensable gases in the working fluid were removed through a degassing process, as follows: boiling of the working fluid, freezing of the working fluid using liquid nitrogen, and evacuating of NCGs in the chamber using a rotary pump. The whole process was repeated twice. The thermo-physical properties of the working fluid are shown in Table 1. The critical diameter in Table 1 was calculated using the following equation [24]:

Table 1
Thermo-physical properties of HFE-7000 at 25 °C.

HFE-7000	C_p $(kJ/kg \cdot K)$	μ $(mPa \cdot s)$	P_{sat} (bar)	h_{fg} (kJ/kg)
	1.3	1.226	0.716	137.58
	σ (mN/m)	ρ_f (kg/m^3)	ρ_g (kg/m^3)	D_{crit} (mm)
	12.33	1404.5	6.052	1.744

$$D_{crit} = 1.84\sqrt{\frac{\sigma}{g\left(\rho_f - \rho_g\right)}} \quad (1)$$

where σ, g, ρ_f, and ρ_g are the coefficient of surface tension, gravitational acceleration, liquid density, and vapour density, respectively. When the hydraulic diameter of the channel is smaller than the critical diameter, a slug-train unit is formed. In the present study, the hydraulic diameters of the channel were 0.75 mm and 0.5 mm, which were small enough to form the slug-train unit.

2.2. Experimental setup

2.2.1. Experimental apparatus for the thermal performance evaluation

Fig. 9 shows the schematics of the experimental setup used to evaluate the thermal performance of the FPHP. The lengths of the evaporator, adiabatic, and condenser sections were, respectively, 20%, 60%, and 20% of the total length of the FPHP. In the evaporator section, the FPHP was attached to a copper block, which was heated by a film heater made of stainless steel. The film heater was connected to a DC power supply (E3633A, HEWLETT-PACARD) for Joule heating. In the condenser section, the FPHP was attached to another copper block, which was cooled internally by the coolant supplied from a bath circulator (RW-0525 G, JEIO Tech.). The inlet temperature of the coolant was fixed at 20°C. When attaching

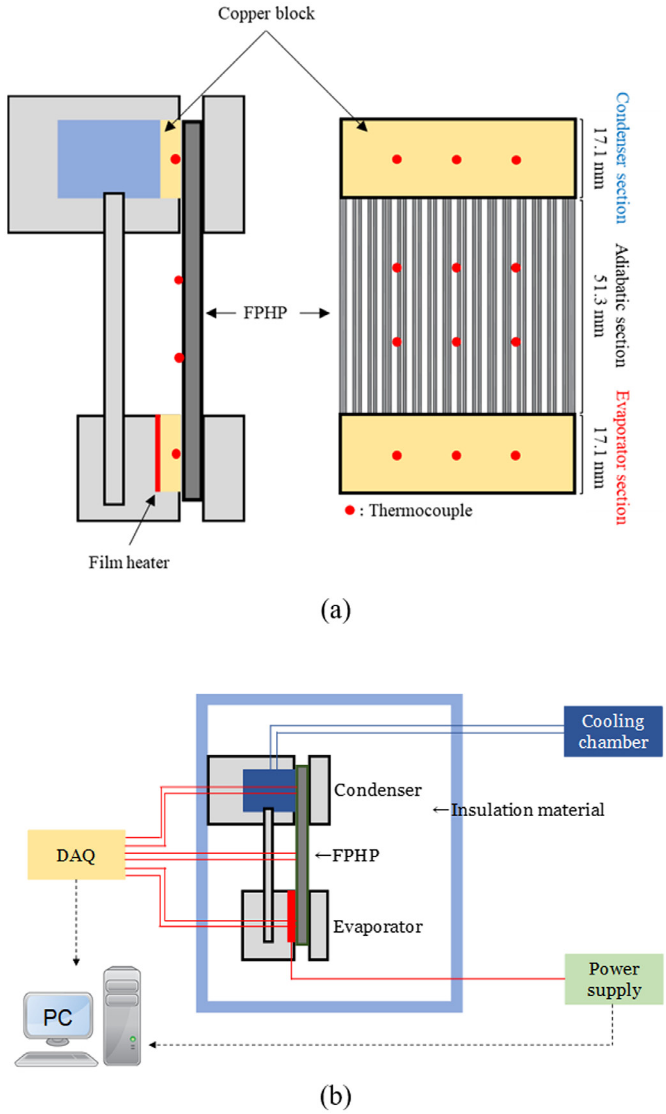

Fig. 9. Schematics of (a) each section and (b) experimental apparatus for evaluating the thermal performance of the FPHP.

the FPHP to the copper blocks, the thermal interface material was used to reduce the contact resistance of the interface between each copper block and the FPHP.

To evaluate the thermal performance of the FPHP, the temperatures were measured using K-type thermocouples. Fig. 9(a) shows locations of thermocouples. The thermocouples at the evaporator and condenser sections were attached to the grooved surface of the copper block using silver epoxy. The temperatures measured from these thermocouples were used to calculate the effective thermal conductivity. Also, the thermocouples in the adiabatic section were attached to the wall of the PHP. Temperature data were recorded using a data acquisition system (34970A, HEWLETT-PACKARD). The working range and the accuracy of the experimental instruments are shown in Table 2.

To minimize the heat loss from the FPHP to the environment, a series of experiments were conducted in an acrylic chamber filled with glass wool, as shown in Fig. 9(b). The experiments were conducted at various input powers for three different conditions: vertical orientation, horizontal orientation, and 45-degree bent condition (Fig. 10). Each experiment started with an input power of 3 W and the input power increased by 1 W. The experiments were conducted for 20 min for each input power and stopped when the maximum temperature was over 80°C.

Table 2
Working range and accuracy of experimental instruments.

Instruments	Working range	Accuracy
DC power supply	0–400 V (0–2.6 A)	9.5% (Including heat loss)
Bath circulator	−25 to 150 °C	±0.05 °C
K-type thermocouples	−100 to 1200 °C	±1°C (±0.4 °C)[a]
Vacuum gauge	0.01–110 Pa	±0.077%

[a] Accuracy in the present study (from 20 to 130 °C).

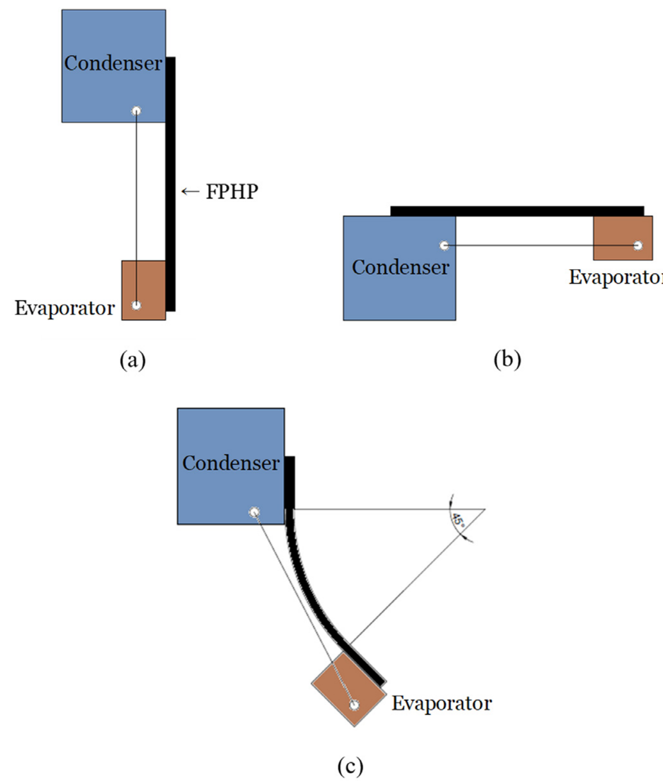

Fig. 10. Schematics of experimental configurations for three conditions: (a) vertical orientation, (b) horizontal orientation, and (c) 45-degree bent condition.

2.2.2. Experimental apparatus for measuring gas permeation through the FPHP

As previously mentioned, permeation of NCGs into the FPHP has a significant impact on the long-term reliability of the FPHP. Therefore, the amount of NCGs permeating into the FPHP was measured to estimate the long-term reliability of the FPHP. For this, the pressure rise method [19] was used. Fig. 11 provides the schematic of the experimental apparatus for measuring the gas permeation rate into the FPHP. The apparatus consisted of stainless steel pipes and a copper block. To minimize any leakage of the system, all the connections in the apparatus were made of VCR (vacuum coupling radiation) fittings containing metallic gaskets. To attach the FPHP specimen to the apparatus, TIG welding was used to join the copper block to the end of the stainless steel pipe. After that, the FPHP specimen was bonded to the copper block by soldering. With the specimen attached, the whole system was evacuated using a turbo pump (TURBOVAC 350iX, Oerlikon). Then, bellows-sealed valve I was closed when the pressure reached 10^{-4} Torr. The internal pressure started to increase because NCGs started to permeate into the system through the FPHP due to a pressure difference. The rate of the pressure increase was measured using a vacuum gauge (CMR 364, Pfeiffer vacuum). The

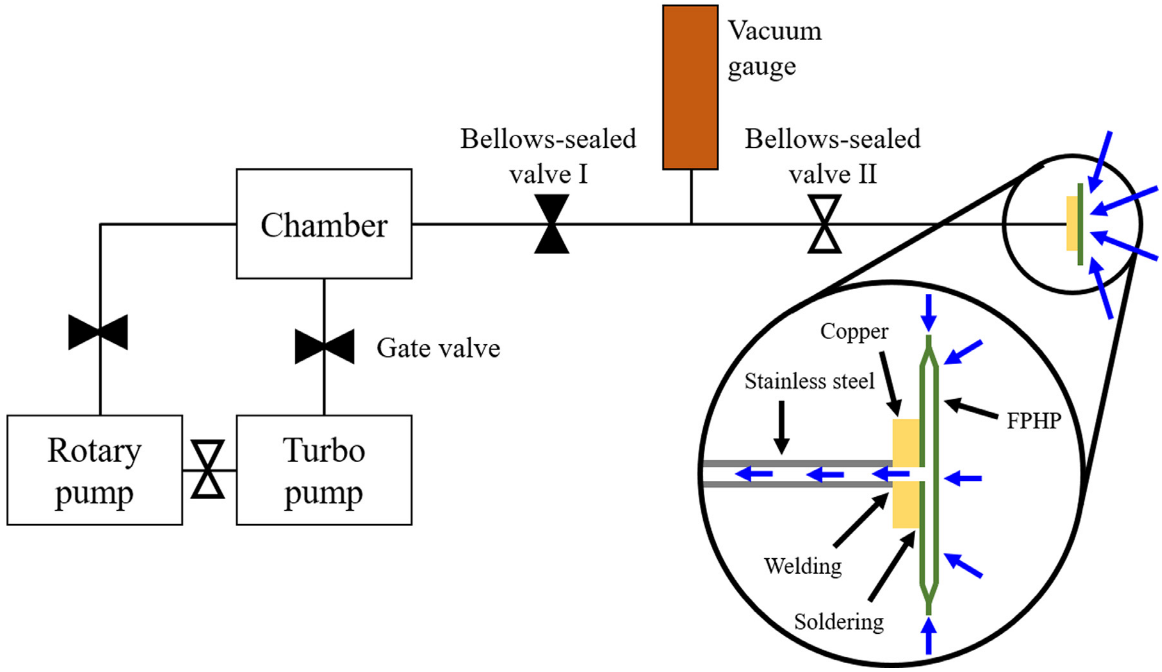

Fig. 11. Schematic of the experimental apparatus for measuring the gas permeability of the FPHP.

working range and accuracy of the vacuum gauge are shown in Table 2. The experiments were performed for two different conditions: vertical orientation and 45-degree bent condition (Fig. 10(a) and (c)).

3. Results and discussion

3.1. Thermal performance of the FPHP

To evaluate the thermal performance of the FPHP, the effective thermal conductivity of the FPHP was calculated using the following equation:

$$k_{\mathrm{eff}} = \frac{Q_{\mathrm{in}} \cdot L_{\mathrm{eff}}}{\left(\overline{T}_e - \overline{T}_c\right) \cdot A_c} \tag{2}$$

where $L_{\mathrm{eff}}, A_c, \overline{T}_e, \overline{T}_c$, and Q_{in} are the effective length and the cross-sectional area of the FPHP, the average temperatures of the evaporator and condenser sections, and the input power, respectively. The representative temperature of each section is the arithmetic average value of the temperature data obtained from the three thermocouples. The time average is obtained from the data after reaching the pseudo-steady state in which the standard deviation of the temperature difference between the evaporator and condenser sections is less than 0.3°C. The effective length and the input power are calculated using the following equations, respectively:

$$L_{\mathrm{eff}} = \frac{L_e + L_c}{2} + L_a \tag{3}$$

$$Q_{\mathrm{in}} = V \times I \tag{4}$$

where L_e, L_c, L_a, V, and I are the lengths of the evaporator, condenser, and adiabatic sections, and the electrical voltage and current, respectively. The experimental uncertainty was analyzed using the method proposed by Holman [25]. In accordance with a 95% confidence interval, the overall uncertainties in the present study were less than 9.5%.

The effective thermal conductivities of the FPHP at various input heat flux in the vertical orientation are presented in Fig. 12.

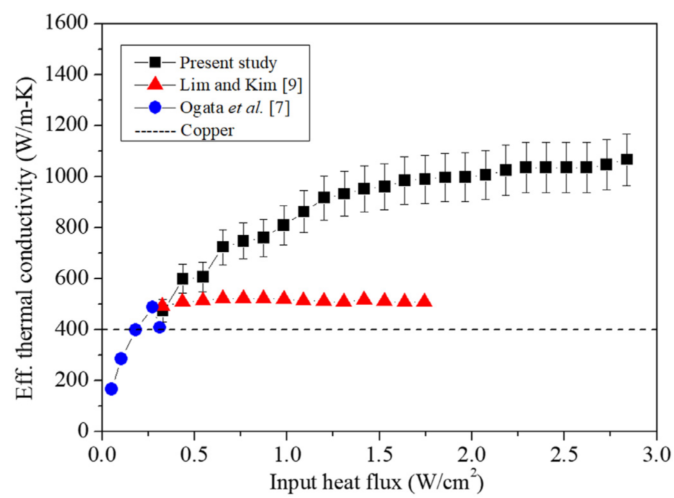

Fig. 12. Effective thermal conductivities of the FPHP at various input heat flux in the vertical orientation.

At an input heat flux of 0.3 W/cm^2, the FPHP starts to operate normally because the startup phenomenon occurs [26]. Then, the experiment was conducted until the input heat flux reached 2.8 W/cm^2, which is approximately 1.6 times higher than that in the previous FPHP [9]. The thermal performance of the FPHP tends to increase with input heat flux, which is in sync with the results reported by Jun and Kim [12]. Accordingly, the FPHP has a maximum effective thermal conductivity of 1070 W/m·K at an input heat flux of 2.8 W/cm^2, which is approximately 2.7 times higher than that of copper and 2 times higher than that of the previous FPHP [9]. The main reason for the improved thermal performance compared to the previous FPHPs is because the bonding process developed in the present study was carried out at room temperature to prevent deformation of the channel geometry. Fig. 13(a) and (c) show the channel geometry before the bonding processes used in the present study and Reference [9] were carried out, respectively. Fig. 13(b) and (d) show the channel geometry after

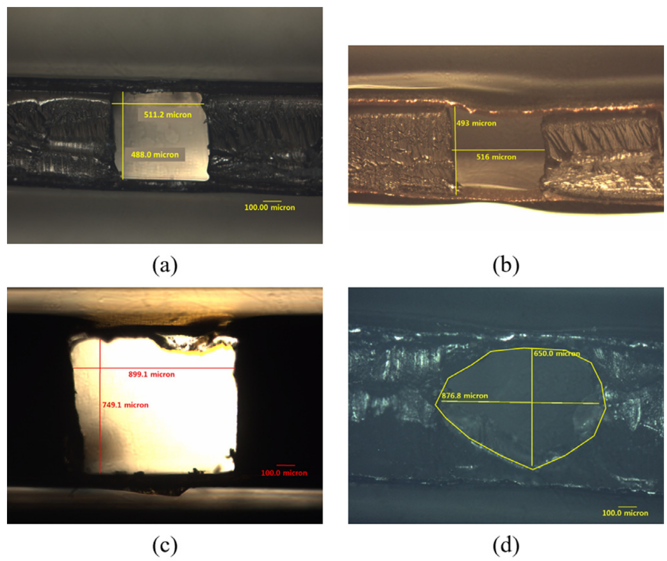

Fig. 13. Microscopic images of the channel geometry of FPHPs: (a) before and (b) after the silane-mediated bonding was carried out, and (c) before and (d) after the thermal bonding was carried out.

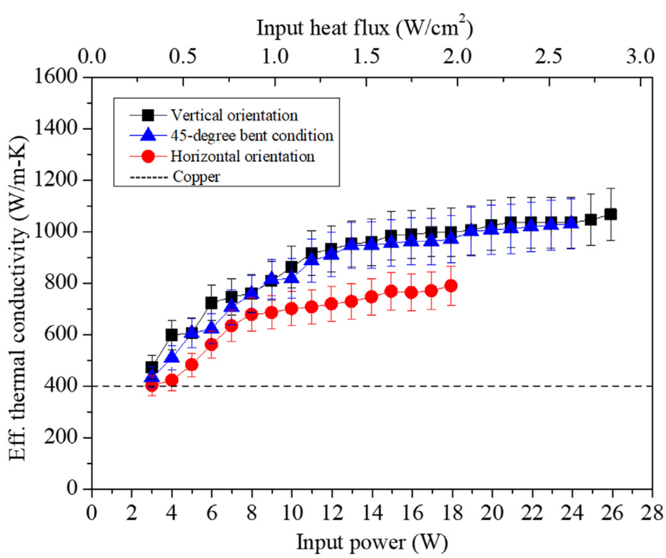

Fig. 14. Effective thermal conductivities of the FPHP at various input powers in three different conditions.

those bonding processes were carried out, respectively. Fig. 13(b) shows the corners of the rectangular channel were maintained without any deformation due to adhesive or melted polymer, while Fig. 13(d) shows the corners of the rectangular channel were partially filled with melted polymer. Lee and Kim [17] reported that the corners of the rectangular channel lead to the thinning of the liquid film along the sides of the channel, resulting in a sharp increase in the heat transfer rate for the phase change process.

Fig. 14 shows the effective thermal conductivities of the FPHP at various input powers for the three different conditions: vertical orientation, horizontal orientation, and 45-degree bent condition. In the vertical orientation, the FPHP has a maximum effective thermal conductivity of 1070 W/m·K at an input power of 26 W, which is 2.7 times higher than that of copper. In addition, it is confirmed that the FPHP works normally even in the horizontal orientation. Generally, it is known that PHPs with less than 20 turns have orientation-dependent performance due to the stopover phenomenon [27]. To solve this problem, a dual-diameter channel [13], which is known to help PHPs achieve orientation-independent performance, was used in the present study. Consequently, although the effective thermal conductivity of the FPHP in the horizontal orientation is decreased by 20.4% on the average compared to that in the vertical orientation, the thermal performance of the FPHP is still higher than that of copper at input powers higher than 3 W. In the 45-degree bent condition, the effective thermal conductivity of the FPHP was maintained well and decreased by only about 3.4% on the average compared to that in the vertical orientation.

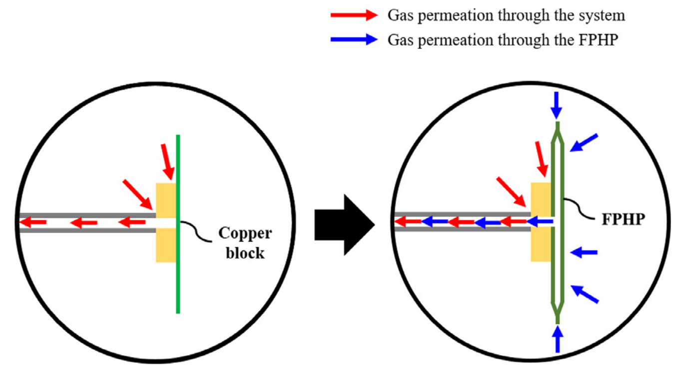

Fig. 15. Experimental process for measuring the gas permeation through the FPHP.

3.2. Long-term reliability of the FPHP

To evaluate the long-term reliability, the gas permeability of the FPHP is measured using the pressure rise method [19]. The rate of the pressure increase inside the FPHP is calculated using the following equation:

$$\left(\frac{dP}{dt}\right)_{\mathrm{FPHP}} = \frac{V_{\mathrm{system}}}{V_{\mathrm{FPHP}}} \cdot \left[\left(\frac{dP}{dt}\right)_{\mathrm{system\ w/\ FPHP}} - \left(\frac{dP}{dt}\right)_{\mathrm{system\ w/o\ FPHP}}\right] \tag{5}$$

where P, V, and$t$are inner pressure, inner volume, and time, respectively. The detailed experimental process is shown in Fig. 15. In order to reduce outgassing inside the system, the whole system was baked in vacuum at 60 °C for 6 h. The rate of the pressure increase was then measured with a copper-foil covering the hole on the copper block first. This measured value corresponds to the amount of NCGs permeating through the system. After that, the rate of the pressure increase was measured again with the FPHP specimen connected to the copper block of the system. In this case, the measured value corresponds to the amount of NCGs permeating through the FPHP as well as through the system. Therefore, the amount of NCGs permeating through the FPHP can be calculated by subtracting the former from the latter.

Fig. 16 shows how the internal pressure increases over the exposure time when the FPHP is in the vertical orientation and 45-degree bent condition. The red dots indicate the values measured with a copper-foil attached to the copper block, which corresponds to the gas permeation through the system itself. Through linear fitting of the data, it can be seen that the rate of the pressure increase is approximately 17.47×10^{-3} Pa/hr. On the other hand, the black dots represent the values measured with the FPHP specimen attached to the copper block of the system. Through linear fitting of the data, it is confirmed that the rate of the pressure increase is approximately 21.07×10^{-3} Pa/hr. Then, by subtracting the former from the latter, the rate of NCGs permeating into the system through the FPHP can be calculated to be approximately 3.6×10^{-3} Pa/hr. Considering that the volume ratio of the system

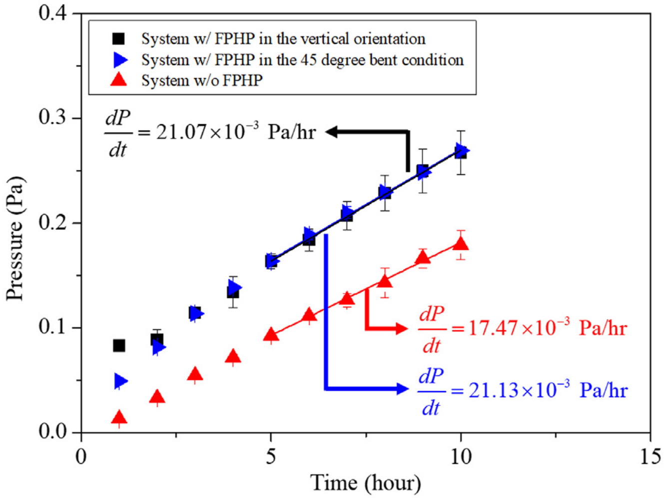

Fig. 16. Rate of the pressure increase of the system and FPHP for air.

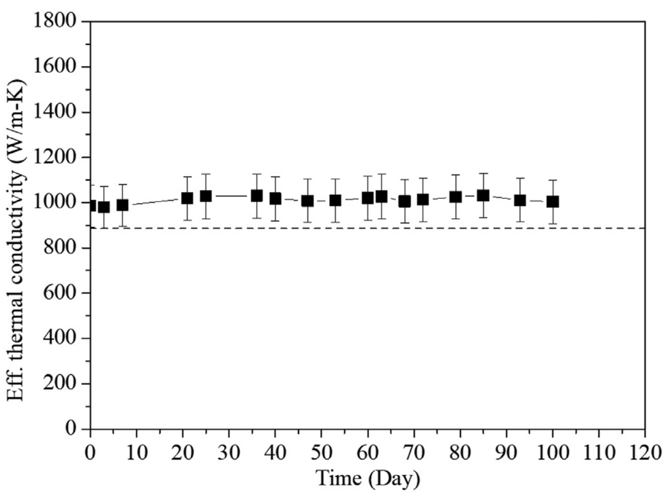

Fig. 17. Change of the thermal performance over the exposure time in an atmospheric-pressure environment at the input power of 15 W.

to the FPHP is 6.3, the rate of NCGs permeating into the FPHP in the vertical orientation can be estimated to be 0.54 Pa/day. Similarly, in the 45-degree bent condition, the rate of NCG permeation can be also estimated to be 0.55 Pa/day using the data obtained from the blue dots in Fig. 16. This implies that the effect of bent condition on the long-term reliability of the FPHP can be negligible. On the other hand, no additional experiment was conducted for the horizontal orientation, since it can be expected the long-term reliability of the FPHP in the horizontal orientation is same as that in the vertical orientation. This is because there is no difference between the former and the latter as far as the gas permeation is concerned. Based on the experimental results reported by Lim and Kim [9], it can be inferred that the pressure of NCGs, which decreases the effective thermal conductivity of the FPHP by 11%, is approximately 2710 Pa, which indicates that the lifetime of the FPHP was at least 2000 days. Therefore, the permeation of NCGs into the FPHP developed in the present study is negligible, which means the issue of the long-term reliability of FPHPs has been practically solved. This improvement is possible because the FPHP is hermetically sealed with metal, such as copper and solder. On the upper and lower sides of the channel, copper-foils with thicknesses of more than 10 μm completely block the permeation of NCGs [28]. So does the soldered copper-foil on the flanges of the FPHP. Because solder has good wettability on the copper surface, there is no effective void, through which NCGs can pass, as shown in Fig. 7.

Additionally, an experiment was conducted to validate the long-term reliability of the FPHP. Fig. 17 shows how the thermal performance of the FPHP changes over the exposure time in an atmospheric-pressure environment at input power of 15 W. The black dotted line indicates the value which is 11% lower than the initial effective thermal conductivity, which is defined as a criterion of the long-term reliability of the FPHP. Over 100 days of measurement, it can be seen that the thermal performance of the FPHP is maintained without any noticeable degradation.

4. Conclusion

In the present study, a method for fabricating a high-performance polymer-based flexible pulsating heat pipe (FPHP) hermetically sealed with metal was proposed, and a series of experiments were conducted to evaluate the thermal performance and long-term reliability of the FPHP. A polycarbonate sheet was used as a base material and a FCCL was used as an envelope. These two materials were bonded together by the silane-mediated bonding method, in which the silane treated surface of PC was chemically bonded to the copper-foil of the FCCL. The flanges were sealed by soldering the two copper-foils; soldering was carried out through tinning of the copper surface and hot-pressing. From the SEM image, it can be confirmed that there was no void at the interface of the joint, which means the FPHP fabricated in this process was hermetically sealed with metal. The width, length, and thickness of the FPHP were 53.4 mm, 85.5 mm, and 0.64 mm. As the working fluid, HFE-7000 was charged into the FPHP.

(a) The thermal performance of the FPHP was evaluated at various input heat powers in three conditions: vertical orientation, horizontal orientation, and 45-degree bent condition. For the vertical orientation, the maximum effective thermal conductivity of the FPHP was 1070 W/m·K. The FPHP operated normally even in the horizontal orientation, and the effective thermal conductivity of the FPHP decreased by 20.4% on the average. In the 45-degree bent condition, the effective thermal conductivity of the FPHP decreased by 3.4% on the average compared to that in the vertical orientation.

(b) The long-term reliability of the FPHP was evaluated by measuring the gas permeability of the FPHP. The rate of the pressure increase inside the FPHP was measured to be approximately 0.54 Pa/day and 0.55 Pa/day in the vertical orientation and 45-degree bent condition, respectively. This indicates that the lifetime of the FPHP was at least 2000 days. Consequently, the issue of the long-term reliability of FPHPs has been practically solved. In addition, to validate the long-term reliability of the FPHP, the thermal performance of the FPHP was measured for 100 days in an atmospheric-pressure environment. It was confirmed that the thermal performance of the FPHP was maintained during that period without any noticeable degradation. The proposed method enables the fabrication of a thin and flexible pulsating heat pipe with high thermal performance and guaranteed long-term reliability.

Declaration of Competing Interest

None.

CRediT authorship contribution statement

Chuljae Jung: Conceptualization, Validation, Formal analysis, Investigation, Resources, Writing - original draft, Writing - review

& editing. **Jonghyun Lim:** Conceptualization, Validation, Investigation, Resources, Writing - original draft. **Sung Jin Kim:** Writing - review & editing, Supervision, Project administration, Funding acquisition.

Acknowledgment

This work was supported by the National Research Foundation of Korea (NRF) grant funded by the Korea government (MSIT) (No. 2012R1A3A2026427).

References

[1] H. Akachi, F. Polášek, P. Štulc, Pulsating heat pipes, in: Proceedings of 5th Int. Heat Pipe Symposium, 1996, pp. 208–217.
[2] Y.H. Lin, S.W. Kang, T.Y. Wu, Fabrication of polydimethylsiloxane (PDMS) pulsating heat pipe, Appl. Therm. Eng. 29 (2009) 573–580.
[3] Y. Ji, G. Liu, H. Ma, G. Li, Y. Sun, An experimental investigation of heat transfer performance in a polydimethylsiloxane (PDMS) oscillating heat pipe, Appl. Therm. Eng. 61 (2013) 690–697.
[4] T. Daimaru, H. Nagai, Operational characteristics of the oscillating heat pipe with non-condensable gas, J. Thermophys. Heat Transfer 29 (2015) 563–571.
[5] R. Senjaya, T. Inoue, Effect of non-condensable gas on the performance of oscillating heat pipe, part I: theoretical study, Appl. Therm. Eng. 73 (2014) 1387–1392.
[6] R. Senjaya, T. Inoue, Effect of non-condensable gas on the performance of oscillating heat pipe, part II: experimental study, Appl. Therm. Eng. 73 (2014) 1393–1400.
[7] S. Ogata, E. Sukegawa, T. Kimura, Performance evaluation of ultra-thin polymer pulsating heat pipes, in: Proceedings of the 14th IEEE ITHERM Conference, 2014, pp. 519–526.
[8] S. Ogata, E. Sukegawa, T. Kimura, Lifetime evaluation of ultra-thin polymer pulsating heat pipe, in: Proceedings of International CPMT Symposium Japan, IEEE, 2014, pp. 15–18.
[9] J. Lim, S.J. Kim, Fabrication and experimental evaluation of a polymer-based flexible pulsating heat pipe, Energy Convers. Manage. 156 (2018) 358–364.
[10] P. Cheng, S.M. Thompson, J. Boswell, H.B. Ma, An investigation of flat-plate oscillating heat pipes, J. Electron. Packag. 132 (4) (2010) 0410094.
[11] S.M. Thompson, P. Cheng, H.B. Ma, An experimental investigation of a three--dimensional flat-plate oscillating heat pipe with staggered microchannels, Int. J. Heat Mass Transfer 54 (2011) 3951–3959.
[12] S. Jun, S.J. Kim, Comparison of the thermal performances and flow characteristics between closed-loop and closed-end micro pulsating heat pipes, Int J. Heat Mass Transfer 96 (2016) 890–901.
[13] G.H. Kwon, S.J. Kim, Experimental investigation on the thermal performance of a micro pulsating heat pipe with a dual-diameter channel, Int. J. Heat Mass Transfer 89 (2015) 817–828.
[14] M.E. Vlachopoulou, A. Tserepi, P. Pavli, P. Argitis, M. Sanopoulou, K. Misiakos, A low temperature surface modification assisted method for bonding plastic substrates, J. Micromech. Microeng. (2009) 19.
[15] K. Aran, L.A. Sasso, N. Kamdar, J.D. Zahn, Irreversible, direct bonding of nanoporous polymer membranes to PDMS or glass microdevices, Lap Chip 10 (2010) 548–552.
[16] H. Yang, S. Khandekar, M. Groll, Performance characteristics of pulsating heat pipes as integral thermal spreaders, Int. J. Therm. Sci. 48 (2009) 815–824.
[17] J. Lee, S.J. Kim, Effect of channel geometry on the operating limit of micro pulsating heat pipes, Int. J. Heat Mass Transfer 107 (2017) 204–212.
[18] P. Charoensawan, P. Terdtoon, Thermal performance of horizontal closed-loop oscillating heat pipes, Appl. Therm. Eng. 28 (5) (2008) 460–466.
[19] H. Jung, C.H. Jang, I.S. Yeo, T.H. Song, Investigation of gas permeation through Al-metallized film for vacuum insulation panels, Int. J. Heat Mass Transfer 56 (2013) 436–446.
[20] K.S. Lee, R.J. Ram, Plastic–PDMS bonding for high pressure hydrolytically stable active microfluidics, Lab Chip 9 (2009) 1618–1624.
[21] S.J. Kim, C. Jung, J. Lim, A flexible flat-plate pulsating heat pipe and manufacturing method thereof, 2019, 10-2019-0001055.
[22] K.J. Rothschild, The early development and application of FTIR difference spectroscopy to membrane proteins: a personal perspective, Biomed. Spectrosc. Imaging 5 (2016) 231–267.
[23] G. Laroche, J. Fitremann, N. Gherardi, FTIR-ATR spectroscopy in thin film studies: the importance of sampling depth and deposition substrate, Appl. Surf. Sci. 273 (2013) 632–637.
[24] M. Hosoda, S. Nishio, R. Shirakasi, Meandering closed loop pulsating heat transport tube, in: Proceedings of the 5th ASME and JSME Thermal Engineering Joint Conference, 1999.
[25] J.P. Holman, Experimental Methods For Engineers, 7th ed, McGraw-Hill, New York, 2001.
[26] W. Qu, H.B. Ma, Theoretical analysis of startup of a pulsating heat pipe, Int. J. Heat Mass Transfer 50 (2007) 2309–2316.
[27] S. Jun, S.J. Kim, Experimental study on a criterion for normal operation of pulsating heat pipes in a horizontal orientation, Int. J. Heat Mass Transfer 137 (2019) 1064–1075.
[28] I. Yeo, H. Jung, T.H. Song, Gas permeation characteristics through heat-sealed flanges of vacuum insulation panels, Vacuum 10 (2014) 70–76.